

Spectroscopically Determined Molecular Mechanics Model for the Intermolecular Interactions in Hydrogen-Bonded Formic Acid Dimer Structures

Weili Qian and Samuel Krimm*

Biophysics Research Division and Department of Physics, University of Michigan, Ann Arbor, Michigan 48109

Received: January 4, 2001

A molecular mechanics (MM) energy function has been optimized for the seven ab initio hydrogen-bonded structures of the formic acid dimer (FAD). Intermolecular interactions are represented by atomic charges, atomic dipoles, and charge fluxes in addition to the van der Waals terms. Intramolecular force constants are optimized by the analytic SDFP procedure. Ab initio MP2/6-311++G** structures, interaction energies, MP2/6-31+G* normal-mode frequencies, and other properties are very well reproduced, indicating that such a nonbonded interaction model can serve as an appropriate representation of the hydrogen-bonding contribution not only for the FAD but in MM functions of other hydrogen-bonded systems.

Introduction

In the context of developing an explicit description for a spectroscopically reliable hydrogen-bond potential in molecular mechanics (MM) energy functions, we have shown^{1,2} that this objective is achievable by using an electrostatic model that incorporates atomic dipoles in addition to the usual atomic charges and van der Waals interactions. Because these studies focused on the intermolecular interactions, the parameter optimization was performed at ab initio structures and intramolecular force constants. This approach was based on the assumption that small residual gradients in the optimization would not cause significant geometry changes in a real MM application. Although this may be true for intramolecular geometries, the intermolecular interaction potential surface may be so flat that such small forces could cause nontrivial intermolecular structure changes. It then becomes important in obtaining a correct structure to reduce all forces to (or close to) zero, i.e., to do a complete MM optimization. We found this to be the case for the *N*-methylacetamide (NMA) dimer,³ and we now extend this approach to the formic acid dimer (FAD).

The MM potential function that we use is a spectroscopically determined force field (SDFP). In such a force field, ab initio structures and experimentally scaled force constants are analytically transformed, using initial values of nonbonded parameters, into an MM energy function.⁴ The protocol, involving subsequent optimization of nonbonded parameters,⁵ thus incorporates frequency agreement (to spectroscopic criteria, viz., rms errors of $\sim 10\text{ cm}^{-1}$) in the initial parametrization. The procedure has been successfully implemented for isolated alkane^{6,7} and alkene⁸ molecules. In this study, as with NMA,³ we extend it to the FAD, with special emphasis on the intermolecular interaction parameters, so as to reproduce the optimized structures, interaction energies, normal-mode frequencies, and other properties of the dimer.

The goal of an SDFP for macromolecules^{6–8} is to have a single transferable force field (which can include conformation-dependent off-diagonal valence force constants) that will account for properties of different chain conformations. To achieve this, the transformation is applied to stable conformers of relevant model molecules, and the optimization is done to a single set of intrinsic force constants and geometry parameters. In the

present study of the FAD, we examine the extent to which a single set of parameters can account not only for the properties of the most stable dimer structure⁹ but also for those of the other six stationary structures found in an ab initio study¹⁰ (see Figure 1). Of course, the situation here is very different from the hydrocarbon case because in the FAD dimers we encounter different kinds of intermolecular (primarily hydrogen-bond) interactions in the seven structures. This poses some possible additional problems. If polarization (which we do not include here) is important, then a set of fixed charges and atomic dipoles will not properly represent the electrostatic component of the intermolecular interactions in all seven FAD structures. Also, if electronic structural differences other than those attributable to polarization occur between different hydrogen-bonded structures, then subtle variations in intrinsic force constants or geometry parameters will be missed. In this connection, although we include cubic and quartic anharmonicity effects on force constants,^{7,8} this may not be sufficient to account for all changes in bond lengths and effective force constants. Despite these potential limitations, it is nevertheless instructive to learn how good the present model is, particularly with respect to the intermolecular interactions of the hydrogen bond.^{1,2} In fact, such a study can reveal insufficiencies in the energy function and point the way to the physical factors that must be included if spectroscopic reproducibility is to be achieved.

It should be noted that although an intermolecular potential has been proposed for the FAD,¹¹ it needs to be emphasized that in this method, based on perturbation theory, rigid monomer structures are used. Although such a simplification makes it possible to separate the inter- from the intramolecular potential function, it is clear that an intermolecular potential derived using rigid molecules cannot be a possible model for an MM energy function. Because, in particular, our SDFP is designed to reproduce vibrational frequencies, it is necessary, as has been realized,¹² that fully optimized dimer structures be used.

Calculations

Ab Initio. All ab initio calculations were done at the MP2 level,¹³ using GAUSSIAN 94.¹⁴ To determine the effect of the frozen core approximation on the intermolecular interaction energy, full and frozen core calculations were done on the

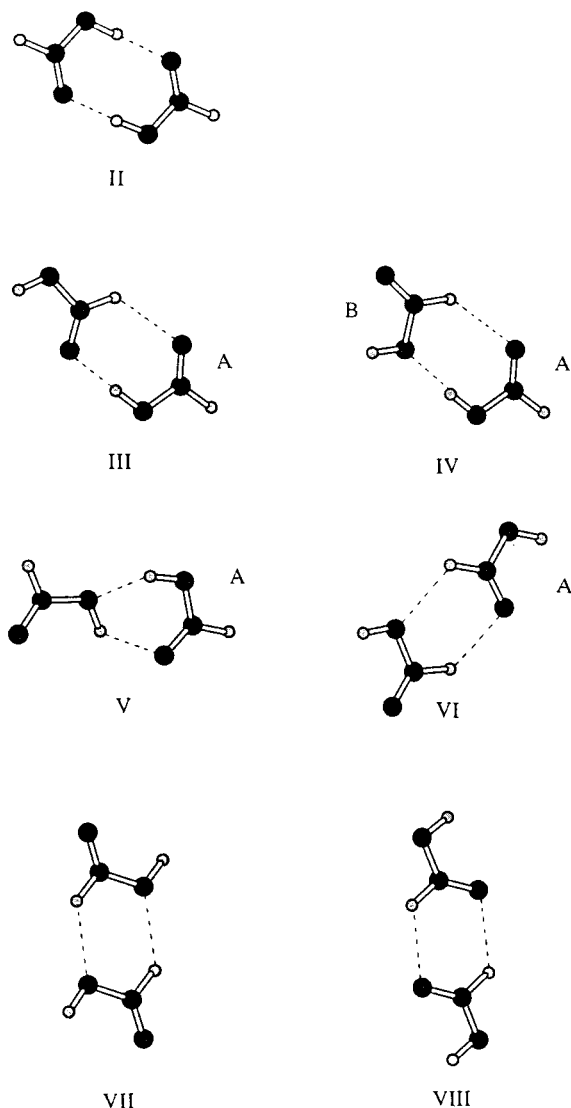


Figure 1. Fully optimized MP2/6-31+G* structures of the formic acid dimer.

monomer and structure **II** (Figure 1) with the 6-311++G** basis set. Although, as expected, the absolute energy differences are quite large, the relative full and frozen core energies are essentially the same (within about 0.01 kcal/mol). We therefore used the frozen core option in all calculations.

To investigate the effect of basis set, dimer structure optimizations and normal mode calculations were done using basis sets from 6-31G* to 6-311++G**. When the geometry optimization is done in the default option of GAUSSIAN (i.e., without using analytical Hessians), all structures are planar if the starting structures are planar. However, if any of these planar structures has an imaginary frequency, this is an indication that the structure is not at a minimum. Thus, at 6-31G*, we find that planar structure **V** has a frequency of 20i cm⁻¹, and further energy minimization starting from a nonplanar structure leads, as noted,¹⁰ to a nonplanar minimum structure. When the basis set is enlarged to 6-31+G* (which results in a planar peptide group in NMA¹⁵), all FAD structures are planar even if the starting structures are nonplanar. When the basis set is enlarged further, some structures become nonplanar. For example, the following planar structures have imaginary frequencies: **IV** - 23i, 161i, and 116i cm⁻¹ at 6-31+G**, 6-311+G*, and 6-311++G**, respectively; at 6-311++G**, **V** - 57i, **VI** - 39i, and **VII** - 19i and 99i cm⁻¹. Basis set convergence, as

TABLE 1: Intermolecular Interaction Energies and Structure Parameters of Formic Acid Dimer Structures

structure ^a	E ^b	X ^c	Y ^c	Z ^c	φ ^c	θ ^c	ψ ^c
II	-13.64	1.41	3.50	0.0	180	0	0
	-14.48	1.43	3.64	0.0	180	0	0
	-13.53	1.41	3.48	0.0	180	0	0
III	-7.79	1.20	3.50	0.0	81.4	180	0
	-8.55	1.18	3.53	0.0	82.4	180	0
	-7.86	1.20	3.39	0.0	83.4	180	0
IV	-5.39	1.10	3.79	0.0	46.3	0	0
	-5.74	1.09	3.77	0.0	45.1	0	0
	-5.95	0.98	3.54	0.0	37.5	0	0
V	-6.28	1.50	4.23	0.0	-99.3	180	0
	-6.92	1.55	4.21	0.0	-100.2	180	0
	-6.10	0.54	4.34	0.0	-73.5	180	0
VI	-2.55	-3.72	-0.42	0.0	-53.0	180	0
	-2.70	-3.69	-0.41	0.0	-53.6	180	0
	-2.72	-3.71	0.35	0.0	-81.6	180	0
VII	-1.93	2.10	-3.35	0.0	180	0	0
	-2.07	2.08	-3.30	0.0	180	0	0
	-1.87	1.79	-3.34	0.0	180	0	0
VIII	-3.15	-3.49	-0.62	0.0	180	0	0
	-3.56	-3.47	-0.62	0.0	180	0	0
	-3.23	-3.44	-0.73	0.0	180	0	0

^a See Figure 1. ^b Energy in kcal/mol. First line: MP2/6-311++G**; second line: MP2/6-31+G*; third line: molecular mechanics. ^c See text for definition of coordinate system translation (X, Y, Z in Å) and Euler angle rotation (φ, θ, ψ in degrees) parameters.

determined from an interaction energy study,¹⁶ only occurs around the much larger cc-pV5Z, but full geometry optimization and normal mode calculations are not feasible at this time with such a basis set. Because the (possibly true) nonplanar structures, probably involving weak C-H...O hydrogen bonds, are not well-characterized at present, and are in any case very sensitive to the MM function³, we have chosen at this stage to use the planar minimum structures at the 6-31+G* level in our ab initio calculations.

Because we define the MM interaction energy by the nonbonded interactions between the monomers in the fully optimized dimer structure, we calculate the ab initio interaction energy as $E = E_{AB}(AB) - 2E_A(AB)$. In this expression, $E_{AB}(AB)$ is the dimer energy at the minimum energy dimer structure and $E_A(AB)$ is the energy of the monomer in the minimized dimer structure using the dimer basis sets. To correct the basis set superposition error (BSSE), the counterpoise method¹⁷ was used for the monomer structure fixed at the optimized dimer structure. We found the 6-311++G** interaction energy of structure **II** (-13.64 kcal/mol) to be close to the cc-pV5Z value (-13.54 kcal/mol) and have, therefore, used these energies in the MM parameter optimization. For comparison, we give these, as well as the 6-31+G*, energies and structures in Table 1 (the structure parameters are defined below).

The intermolecular normal modes are described in terms of the intermolecular coordinates given in Table 2. In contrast to our earlier work,² we do not scale the intermolecular force constants, in order that we may assess the frequency agreement of **II** with experiment² in an unbiased manner. This comparison is shown in Table 3, together with the ab initio intermolecular frequencies and normal modes (including their potential energy distribution, PED) of the structures. The intramolecular internal coordinates are the same as those used previously.² Although the availability of good experimental data for **II** makes determination of its intramolecular force constant scale factors straightforward,² the use of all of these scale factors for the other structures is not justified. This is because, as was found for NMA,¹⁸ the scale factor for a hydrogen-bonded group is

TABLE 2: Intermolecular Internal Coordinates of Formic Acid Dimer Structures

structure ^a	coordinates ^b					
II	O5O10 s	C3O5O10 b	C8O10O5 b	O5O10 t	C3O5 t	C8O10 t
III	O5O10 s	C3O5O10 b	C8O10O5 b	O5O10 t	C3O5 t	C8O10 t
IV	O5O7 s	C3O5O7 b	C8O7O5 b	O5O7 t	C3O5 t	C8O7 t
V	H1H6 s	O2H1H6 b	O7H6H1 b	H1H6 t	O2H1 t	O7H6 t
VI	H4H9 s	C3H4H9 b	C8H9H4 b	H4H9 t	C3H4 t	C8H9 t
VII	H4H9 s	C3H4H9 b	C8H9H4 b	H4H9 t	C3H4 t	C8H9 t
VIII	H4H9 s	C3H4H9 b	C8H9H4 b	H4H9 t	C3H4 t	C8H9 t

^a See Figure 1. ^b s = stretch, b = bend, t = torsion. Atom numbering is based on molecule: A – H1O2C3H4O5, B – H6O7C8H9O10. Torsion coordinate is the average of four-atom coordinates, always including atoms of the intermolecular stretching coordinate. Examples: **II** – O5 O10 t = C3O5...O10C8; C3O5 t = $\frac{1}{2}(\text{H4C3O5}\cdots\text{O10} + \text{O2C3O5}\cdots\text{O10})$. **VI** – C3H4 t = $\frac{1}{2}(\text{O5C3H4}\cdots\text{H6} + \text{O2C3H4}\cdots\text{H6})$.

TABLE 3: Intermolecular MM Frequencies^a and Unscaled ab Initio Frequencies^a and Normal Modes of Formic Acid Dimer Structures

structure ^b	ν^a			mode ^d
	mm ^c	ai ^c	exp ^c	
II	247	254	248	COO ab(106)
	222	243	230	C=O at(226) C–O at(124)
	188	203	190	O5O10 s(86)
	170	170	163	C=O st(262) C–O st(119)
	129	162	137	COO sb(233) O5O10 s(108)
III	25	69	68	O5O10 t(102) C–O st(41)
	187	196		C3O5 t(231) C3O2 t(109)
	165	193		C3O5O10 b(90)
	136	146		O5O10 s(163) C3O5O10 b(109)
	78	106		C8O10O5 b(83)
IV	75	101		C8O10 t(122)
	28	60		O5O10 t(144)
	160	170		C3O5O7 b(96)
	160	157		C3O5 t(186) C3O2 t(70)
	137	137		O5O7 s(133) C3O5O7 b(79) C8O7O5 b(35)
V	99	95		C8O7O5 b(72) O5O7 s(44) C3O5O7 b(24)
	84	88		C8O7 t(55) O5O7 t(15)
	41	27		O5O7 t(129) C8O7 t(85)
	237	224		H1H6 s(25) O2H1H6 b(23)
	151	172		O2H1 t(121) H1H6 t(65) C8O7 t(28)
VI	97	145		H1H6 t(127) C3O2 t(30) C8O7 t(21)
	86	140		H1H6 s(41) O7H6H1 b(22) O2H1H6 b(16)
	50	74		O2H1H6 b(110) O7H6H1 b(94)
	16	21		O7H6 t(165) H1H6 t(22)
	98	91		H4H9 t(52) C3H4 t(21)
VII	95	90		C3H4H9 b(41) H4H9 s(18)
	71	81		H4H9 s(157) C8H9H4 b(86) C3H4H9 b(48)
	41	74		C3H4H9 b(77) C8H9H4 b(48) H4H9 s(33)
	23	56		C3H4 t(66) H4H9 t(43) C8H9 t(42)
	12	25		C8H9 t(62) C3H4 t(42) H4H9 t(33)
VIII	92	80		CHH sb(44) H4H9 s(16)
	70	72		H4H9 s(195) CHH sb(165)
	67	72		CHH ab(102)
	63	64		H4H9 t(82)
	34	50		CH at(101)
IX	24	16		CH st(223) H4H9 t(138)
	94	97		CHH sb(62)
	89	96		H4H9 t(85)
	76	86		H4H9 s(199) CHH sb(139)
	51	80		CHH ab(101)
X	29	79		CH at(99)
	22	33		CH st(113) H4H9 t(26)

^a In cm^{-1} . ^b See Figure 1. ^c mm = molecular mechanics, ai = ab initio, exp = experimental (see ref 2). ^d ab, sb = antisymmetric, symmetric bend; at, st = antisymmetric, symmetric torsion; s = stretch; t = torsion; C8O7 t, C3O2 t = intramolecular coordinates (see ref 2). Main components of potential energy distribution.

not the same as that for the free group. We have taken account of this difficulty as follows. Ab initio vibrational calculations

TABLE 4: Intramolecular Force Constant Scale Factors for Formic Acid Dimer Structures

coordinate ^a	scale factor			
	optimized ^b		applied	
	monomer	II	value	structure
CH s	0.8567	0.8585	0.8585	II
			0.8576	all others
OH s	0.9520	0.8544	0.8544	II, IIIA, IVA, VB
			0.9032	IVB, VA
C=O s	0.9816	0.9396	0.9520	IIIB, VIA, VIB, VII, VIII
			0.9396	II, IIIB, VA
			0.9606	IIIA, IVA, VIA, VIII
C–O s	0.9249	0.9604	0.9816	IVB, VB, VIB, VII
			0.9604	II, IIIA
			0.9427	IVA, VA
			0.9249	IIIB, IVB, VB, VIA, VIB, VII, VIII
HC=O b	0.9396	0.9502	0.9502	II
			0.9449	all others
OCO b	1.0689	1.0802	1.0689	II
			1.0746	all others
COH b	0.9758	0.9148	0.9148	II, IIIA
			0.9453	IVA, VA
			0.9758	IIIB, IVB, VB, VIA, VIB, VII, VIII
CH ob	0.9621	0.9625	0.9625	II
			0.9623	all others
C–O t	0.8633	0.9000	0.9000	II
			0.8817	all others

^a s = stretch, b = bend, ob = out-of-plane bend, t = torsion. ^b Optimized to experimental frequencies: monomer – ref 12, dimer structure II – ref 2.

were done for all isotopic derivatives of the monomer and scale factors were determined to reproduce the experimental frequencies.¹² (The rms error between observed and such calculated frequencies below 1800 cm^{-1} is 5.8 cm^{-1} , 3.1 cm^{-1} for HCOOH, with the supposed 1223 cm^{-1} COH bend (b) band¹² given zero weight in the optimization since its existence has not been confirmed.¹⁹) For those coordinates for which the difference in scale factors was small, the average value of the **II** and monomer values was used for all structures other than **II**. For those cases in which there was a large difference, e.g., OH stretch (s), the monomer value was used for the structures with free groups, the **II** value was used where the strongly bonded group occurred, and the average value was used for intermediate cases. All of these scale factors are given in Table 4. The resulting scaled intramolecular modes are given in Table 5.

Molecular Mechanics. The intermolecular MM potential energy model was the same as that used previously.^{1,2} On the basis of our earlier work,⁹ we use dipole-derivative derived charges²⁰ (DDC) for the initial charge values because these can be obtained directly from ab initio dipole derivatives. The advantages of the DDC, which have also been called effective²¹

TABLE 5: Intramolecular MM and Scaled ab Initio Frequencies^a of Formic Acid Dimer Structures

structure ^b		mode ^c								
		OH s	CH s	C=O s	CH b	COH b	C-O s	CH ob	C-O t	OCO b
II	a	3040	2957	1747	1406	1313	1170	1063	872	688
		3110	2951	1730	1412	1358	1217	1053	889	694
		3110	2949	1741		1362	1217	1060		699
	s	3039	2956	1705	1404	1368	1168	1064	927	676
		3043	2954	1679	1417	1374	1217	1066	924	678
III	A	3111	2951	1754	1403	1335	1155	1051	780	669
		3163	2931	1744	1407	1347	1188	1047	868	674
	B	3570	2961	1718	1401	1293	1144	1056	651	654
		3561	2983	1706	1382	1301	1129	1070	667	646
		3190	2955	1747	1404	1338	1147	1042	779	667
IV	A	3281	2937	1746	1410	1345	1169	1042	793	666
		3430	2963	1758	1399	1291	1060	1048	662	641
	B	3479	2978	1784	1385	1256	1064	1045	609	623
		3464	2967	1735	1403	1344	1143	1055	654	667
		3398	2952	1724	1412	1349	1167	1045	731	681
V	A	2996	2960	1758	1399	1288	1112	1043	800	658
		3241	2934	1783	1389	1284	1107	1031	816	644
	B	3557	2947	1746	1399	1293	1133	1045	664	648
		3566	2967	1750	1387	1295	1112	1048	655	630
		3566	2961	1757	1405	1291	1110	1048	654	644
VI	A	3569	2975	1774	1394	1273	1087	1051	640	623
		3506	2958	1752	1398	1293	1118	1044	675	645
	s	3569	2969	1773	1386	1284	1099	1044	641	625
		3533	2958	1765	1403	1292	1098	1043	656	643
		3570	2974	1779	1400	1267	1082	1042	635	623
VII	a	3577	2955	1756	1401	1291	1120	1052	659	646
		3565	2970	1752	1387	1293	1100	1057	657	631
	s	3577	2955	1738	1403	1292	1140	1050	652	646
		3565	2973	1738	1387	1294	1118	1057	654	628
		3577	2955	1738	1403	1292	1140	1050	652	646

^a In cm^{-1} . ^b See Figure 1. a = antisymmetric, s = symmetric. ^c Main component of potential energy distribution. s = stretch, b = bend, ob = out-of-plane bend, t = torsion (see ref 2 for definition of coordinates). First line in entry: molecular mechanics value; second line: scaled ab initio value; third line (for structure II): experimental value (see ref 2).

and force related²² charges, is that they are uniquely calculable for planar molecules, they exactly reproduce the molecular dipole moment and the dipole derivatives, and they are the charges that govern long-range interactions.²⁰ We do not use atomic dipoles from quadrupole derivatives⁹ but treat them as adjustable parameters, with dipole moments only on the heavy atoms and directed along bonds. Both the charges and the dipoles are adjusted during the optimization procedure. The van der Waals parameters that we used in our earlier work²³ were wrong,²⁴ and we have used the corrected values²⁴ as starting points in the present study, again because they work well in predicting thermodynamic properties of liquid formic acid.²⁵

The intramolecular parameters were obtained by the analytic SDFP transformation,⁴ using the SPEAR program²⁶ for energy minimization and parameter optimization. Consistent with the standard SDFP philosophy,^{5,6} all intramolecular force constants at this stage were kept the same in all structures. However, to obtain comparable frequency agreement, the C-O torsion (t) force constant had to be treated differently, which reveals a possibly important physical property of this coordinate in MM functions. The problem arises from the significantly different observed frequencies of this mode in the monomer (642 cm^{-1})¹² and in dimer II (923 cm^{-1}).² Because the C-O t force constant derives from a (in our case one-term) torsion potential, the above 44% difference in frequencies translates into a very large difference in the barriers associated with the respective potentials. Because ab initio C-O t frequencies of some structures fall in the range of that of the monomer (see Table 5), it is clear that a single barrier will not suffice to describe the C-O t modes of all structures. At this stage, we have chosen to optimize the barrier for structure II to its experimental and scaled ab initio torsion frequencies (which results in a value of 8.5

kcal/mol) and to optimize a single value of the barrier for all the other structures (which results in a value of 4.9 kcal/mol). (We discuss below how this approach could be improved.) This is not unreasonable: structure II is special not only in having two strong O-H...O=C hydrogen bonds but in exhibiting proton transfer in the two hydrogen bonds via tunneling.²⁷ This may well be associated with an exceptionally high C-O t barrier and frequency.

The structures of the dimers are described by the three components of the translation and the three Euler angles that relate the local coordinate system of molecule B (see Figure 1) with respect to that of molecule A. We take the origin at the C atom of A, the X axis along the C-O(H) bond, and the Y axis pointing near the C=O direction. The ϕ rotation is about the Z axis, the θ rotation is about the X axis, and the ψ rotation is about the shifted Z axis.

The optimization procedure was as follows. Using the initial van der Waals and charge parameters, the valence-type intrinsic force constant and geometry parameters were obtained from the SDFP transformation.⁴ Initial atomic dipole parameters were obtained by a grid search technique. In this method, the geometry, interaction energy, and normal-mode frequencies were optimized to the corresponding ab initio values for the seven structures in the context of assigning the best initial atomic dipole parameters. It should be noted that the effective atomic charges are partly determined by charge fluxes, arising from geometry changes in the seven structures, and such charge fluxes also need to be optimized. Also, atomic dipole moments contribute to molecular dipole derivatives. Thus, in later stages of the parameter refinement, ab initio molecular dipole derivatives as well as some normal-mode frequency splittings were also used to refine atomic charges and charge fluxes. Using

TABLE 6: Molecular Mechanics Intermolecular Interaction Parameters for Formic Acid Dimer Structures

atom or bond	parameter					
	A ^a	B ^a	Q ^b	dq/dr ^c	m ₁ ^d	m ₂ ^e
H(O)	0.265	0.342				
O(H)	644.64	18.80				
C	1654.60	28.20				
H(C)	0.036	0.071				
O(C)	391.09	19.66				
CH/CH			0.0849		0.1208	
CH/C–O				0.1890		
OH/OH			0.3364	0.7000	0.0758	
OH/COH				0.0390		
C–O/C–O			–0.0779	–0.7000	0.0439	
C–O/OH				–0.0080		
C–O/C=O				0.0700		
C–O/COH				–0.0580		
C–O/O–CH				0.0083		
C–O/O=CH				–0.0280		
C–O/OCO				–0.0056		
C=O/C=O			–0.4437	–0.8500		0.0914

^a Parameter in van der Waals potential: $A r^{-12} - B r^{-6}$. ^b Dipole-derivative derived atomic charge in terms of bond charge increment. ab: a – negative, b – positive; units: fractional electron charges. ^c Charge flux (in electrons/Å or electron/rad). ab/cd(e): charge flux in bond ab (sign convention as in footnote b) due to change in coordinate cd or cde. ^d Atomic dipole on atom a, directed along ab. Units: electron charge·Å. ^e Atomic dipole on atom b, directed along ab. Units: electron charge·Å.

manual as well as automatic optimization programs, our goal was to find a maximally consistent set of parameters that would simultaneously fit the ab initio structures, intermolecular interaction energies, dipole derivatives, and normal-mode frequencies of all seven stationary FAD structures. The resulting parameters are given in Table 6, the MM structures and energies are given in Table 1, and the scaled ab initio and the MM normal-mode frequencies are compared in Tables 3 and 5.

Results and Discussion

Before considering the MM results in detail, it is useful to examine some characteristics of the ab initio properties of the seven structures. This can provide insights into possible requirements on MM models designed for spectroscopic accuracy.

Ab Initio. With respect to the intermolecular interactions, we note the wide range of interaction energies, from 13.64 kcal/mol for **II** to 1.93 kcal/mol for **VII** (Table 1). This primarily reflects the wide range of hydrogen-bond strengths in these structures, from two O–H···O= bonds in **II** to two C–H···O– interactions in **VII**. As would be expected, the intermolecular frequencies, on average, generally follow this trend (see Table 3), although individual modes are not expected to do so because their eigenvectors are not exactly the same. The challenge for a complete intermolecular SDFP potential is, of course, to reproduce these energies and individual frequencies with reasonable accuracy, thus validating the model as a useful description of the hydrogen-bond interaction. At this stage, we should certainly expect it to at least reproduce significant trends in these quantities, and particularly, the large differences in frequencies between the structures: from 254 cm⁻¹ in **II** to 80 cm⁻¹ in **VII** for the highest intermolecular frequency and from 69 cm⁻¹ in **II** to 16 cm⁻¹ in **VII** for the lowest intermolecular frequency.

The intramolecular data reveal an analogous range of properties that provide a basic challenge to an MM description. To make this clearer, we present in Table 7 unscaled ab initio data for some of the normal modes of the dimer structures. As

expected, the force constants, f , vary almost linearly with bond length, r , for OH s, CH s, and C=O s. For OH s, this varies from $f(\text{OH}) \cong 7.5$ mdyn/Å at $r(\text{OH}) \cong 0.982$ Å for the free OH groups (**IIIB**, **IVB**, **VI**, **VIB**, **VII**, and **VIII**, and including the monomer with $f = 7.4945$ at $r = 0.9820$) to $f(\text{OH}) \cong 6.2$ mdyn/Å at $r(\text{OH}) \cong 1.000$ Å for the strongly bonded OH groups of **II**. For CH s, a similar almost linear relationship is found, from $f(\text{CH}) \cong 5.68$ mdyn/Å at $r(\text{CH}) \cong 1.093$ Å for the strongly bonded CH···O=C of **IIIB** to $f(\text{CH}) \cong 5.51$ mdyn/Å at $r(\text{CH}) \cong 1.096$ Å for the free CH of **IIIA**. For C=O s, the relation is less obvious, but this is somewhat artifactual. If instead of obtaining internal coordinate force constants by transforming ab initio Cartesian force constants by an A-matrix of the full internal (i.e., inter- plus intramolecular) coordinates (as was done for Table 7), which gives force constants that depend on the definitions of the intermolecular coordinates, we use an A-matrix of the intramolecular coordinates only, we obtain a set of intramolecular force constants that is self-consistent across all of the structures. Although this alternative transformation has little effect for OH s (the only significant change is that $f(\text{OH})$ of **VA** becomes 7.1533, bringing it close to the linear relation) or CH s (essentially no change), it does account for large changes in some $f(\text{C=O})$ (to 13.4737 for **IVB**, 12.7532 for **IIIA**, and 12.3610 for **II**), all of which combine to yield an essentially linear $f(\text{C=O})/r(\text{C=O})$ relation. The situation with C–O t is that such a relation is only evident with the alternative transformation, which yields values of $f(\text{C–O t})$ of 0.3652(**II**), 0.3433 (**IIIA**), 0.2904 (**IVA**), and 0.2636 (**VB**) for structures with bonded OH groups and 0.2097 (**IIIB**), 0.2013 (**VIA**), 0.1741 (**IVB**), 0.2025 (**VIII**), 0.1915 (**VII**), and 0.1935 (**VIB**) for structures with free (or essentially free) OH groups. (The near constancy of $f(\text{C–O t})$ of this latter group with $r(\text{C–O})$, which varies from 1.3411 to 1.3725 Å, seems to indicate that competing influences may be at work.)

The characteristics of CH s and its frequency deserve some attention, particularly in view of the recent interest in C–H···O hydrogen bonding in proteins^{28–30} and from a theoretical perspective.^{31–33} It has seemed that “...spectroscopic evidence for [C–H···O] hydrogen bonding is noticeably absent,”³⁴ but this was probably due to the expectation that, similar to OH and NH hydrogen bonds, the CH s frequency would always be red-shifted on hydrogen bonding. That this need not be the case was demonstrated by the presence of both red- and blue-shifted CH s bands in early studies of the infrared spectrum of polyglycine II^{35,36} and by recent theoretical considerations.³¹ The data of Table 7 clearly show that, in distinction to OH s, C–H···O hydrogen bonding in FAD structures leads to a *decrease* in $r(\text{CH})$ and therefore to a blue-shift in the CH s frequency (we consider a possible simple physical reason for this below). More interesting perhaps is the observation that, in contrast to the constancy of $r(\text{OH})$ for free or weakly CH-bonded OH groups (0.9822 ± 0.0002 Å), the value of $r(\text{CH})$ (and therefore the frequency) for free CH groups varies considerably, from 1.0943 Å (and 3188 cm⁻¹) for **II** to 1.0960 Å (and 3164 cm⁻¹) for **IIIA**. Thus, in distinction to the situation in simpler systems,³¹ we must be prepared for a complex dependence of even a hydrogen-bonded CH s frequency on the intra- as well as intermolecular environment. In searching for whether some characteristic of the intramolecular environment is related to $r(\text{CH})$ of free groups, we find it interesting that there is an essentially linear relationship with $q(\text{–O–}) + q(\text{O=})$, i.e., the sum of charges on the two adjacent O atoms (Figure 2, right-hand side). For the C–H···O=C groups, a similar linear relation holds if we add to these the charge of the ···O = atom (Figure 2, left-hand side). These charge combinations are obviously

TABLE 7: Unscaled ab Initio Data for Some Vibrational Modes of Formic Acid Dimer Structures

parameter ^a	structure ^b						
	II	III	IV	V	VI	VII	VIII
OH s							
A: $\nu(\text{OH})$	3364	3422	3550	3578	3658	3659	3654
$f(\text{OH})$	6.1767	6.5457	7.0574	7.4968	7.4815	7.4979	7.4783
$r(\text{OH})$	1.0003	0.9954	0.9888	0.9876	0.9822	0.9819	0.9822
$r'(\text{OH})$	1.0105	1.0066	1.0003	0.9873	0.9822	0.9847	0.9811
$q(\text{O})$	-0.3755	-0.3954	-0.3982	-0.3895	-0.4164	-0.4176	-0.4178
$q(\text{H})$	0.3463	0.3408	0.3485	0.3564	0.3747	0.3736	0.3732
B: $\nu(\text{OH})$	3291	3650	3661	3503	3655	3658	3654
$f(\text{OH})$		7.4612	7.5085	7.0661	7.4955		
$r(\text{OH})$		0.9826	0.9823	0.9917	0.9819		
$r'(\text{OH})$		0.9815	0.9921	1.0132	0.9818		
$q(\text{O})$		-0.4067	-0.4277	-0.4145	-0.4213		
$q(\text{H})$		0.3775	0.3803	0.3421	0.3720		
CH s							
A: $\nu(\text{CH})$	3188	3164	3170	3186	3202	3206	3206
$f(\text{CH})$	5.5824	5.5096	5.5277	5.5791	5.6384	5.6298	5.6526
$r(\text{CH})$	1.0943	1.0960	1.0956	1.0945	1.0938	1.0935	1.0936
$r'(\text{CH})$	1.0960	1.0955	1.0954	1.0956	1.0955	1.0957	1.0961
$q(\text{C})$	0.2810	0.2598	0.2660	0.2800	0.2774	0.2743	0.2751
$q(\text{H})$	0.1124	0.1131	0.1157	0.1187	0.1270	0.1290	0.1309
B: $\nu(\text{CH})$	3184	3220	3213	3167	3209	3205	3206
$f(\text{CH})$		5.6807	5.6533	5.5123	5.6414		
$r(\text{CH})$		1.0928	1.0932	1.0958	1.0934		
$r'(\text{CH})$		1.0966	1.0959	1.0949	1.0968		
$q(\text{C})$		0.3018	0.2873	0.2944	0.2719		
$q(\text{H})$		0.1359	0.1372	0.1171	0.1328		
C=O s							
A: $\nu(\text{C=O})$	1783	1786	1784	1775	1786	1798	1788
$f(\text{C=O})$	12.7471	13.0423	12.8836	12.6567	13.0455	13.2553	12.9950
$r(\text{C=O})$	1.2312	1.2241	1.2219	1.2248	1.2196	1.2159	1.2205
$r'(\text{C=O})$	1.2301	1.2220	1.2213	1.2254	1.2204	1.2154	1.2208
$q(\text{O})$	-0.3661	-0.3692	-0.3605	-0.3566	-0.3558	-0.3593	-0.3615
B: $\nu(\text{C=O})$	1734	1757	1803	1804	1793	1793	1774
$f(\text{C=O})$		12.8479	13.7523	13.3679	13.2328		
$r(\text{C=O})$		1.2261	1.2129	1.2137	1.2163		
$r'(\text{C=O})$		1.2290	1.2138	1.2150	1.2173		
$q(\text{O})$		-0.3577	-0.3486	-0.3481	-0.3623		
C-O t							
A: $\nu(\text{C-O})$	966	922	844	852	696	681	698
$f(\text{C-O})$	0.4536	0.4202	0.3361	0.2760	0.2007	0.1909	0.2012
$r(\text{C-O})$	1.3263	1.3382	1.3429	1.3413	1.3509	1.3612	1.3518
$r'(\text{C-O})$	1.3398	1.3474	1.3497	1.3476	1.3513	1.3610	1.3525
B: $\nu(\text{C-O})$	935	709	647	758	680	675	695
$f(\text{C-O})$		0.2074	0.1725	0.1677	0.1929		
$r(\text{C-O})$		1.3411	1.3725	1.3579	1.3628		
$r'(\text{C-O})$		1.3459	1.3767	1.3615	1.3597		

^a s = stretch, t = torsion. Frequency, ν , in cm^{-1} . Force constants, f , in $\text{mdyn}/\text{\AA}$. (Internal coordinate force constants were transformed from ab initio Cartesian force constants by the A-matrix for the full internal coordinates. The choice of intermolecular coordinates will affect the intramolecular force constants slightly.) Bond length in \AA ; r - ab initio, r' - MM. Dipole-derivative derived atomic charge, q , in electrons. ^b See Figure 1.

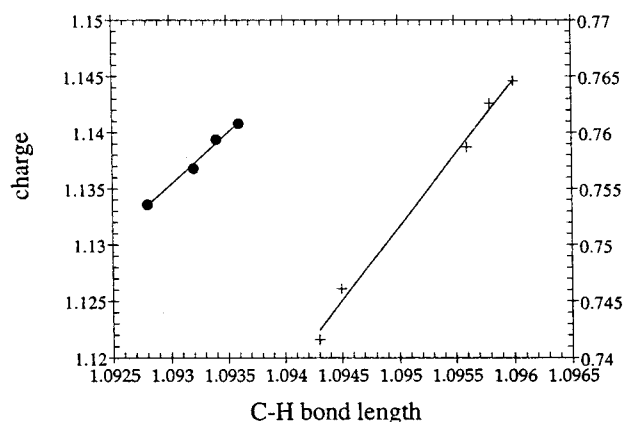


Figure 2. Dependence of C-H bond length (in \AA) on charge parameter (in electrons). + (free CH groups, right-hand scale): charge = negative of $q(\text{-O-}) + q(\text{O=})$; ● (hydrogen-bonded CH groups, left-hand scale): charge = negative of $q(\text{-O-}) + q(\text{O=}) + q(\cdots \text{O=})$.

determined by the specific nature of the hydrogen-bonding interactions between the monomers but the result is consistent

with the observation that the presence of an electronegative group attached to the C atom of a CH group will lead to a shortening of the CH bond.³⁷

Molecular Mechanics. The MM intermolecular interaction energies of the seven FAD structures are given in Table 1, and it can be seen that the agreement with the MP2/6-311++G** values is very good, the rms error being 0.29 kcal/mol. The MM structures, also given in Table 1, are in generally good agreement with the MP2/6-31+G* structures, to which they were optimized, although some structures are more discrepant than others (rms errors are 0.40 \AA in X, 0.31 \AA in Y, and 19.7° in ϕ for nonsymmetry-determined structures). We find that atomic dipoles are crucial to getting even reasonable structure agreement: without them, structures starting from **III**, **V**, and **VI** all optimize to the same structure similar to **III**. It is undoubtedly true that if polarization were included in the electrostatic interactions, the structural agreement, which is fundamental to achieving good intermolecular frequency agreement, would be improved.

The MM intermolecular frequencies are given in Table 3. Although the overall agreement is poorer than our spectroscopic

criterion of $\sim 10 \text{ cm}^{-1}$ (the rms error is 22.1 cm^{-1}), many of its features are encouraging. The general trend of the ab initio frequencies is reproduced, although the MM are mostly lower, particularly the lowest frequencies. The severe discrepancy in the O5O10 t mode of **II** (69 ab initio vs 25 cm^{-1} MM) suggests that an important component may be missing from the intermolecular energy function, and perhaps this is related to the absence of effects due to polarization. Of course, it should be recalled that we have adopted van der Waals parameters that make no distinction between free and bonded (C=O) and H(O) atoms. Such fine details of the van der Waals interactions, including the form of the potential, may be especially important for describing the intermolecular frequencies accurately.

Although the SDFP procedure can drive intramolecular frequency agreement in different conformers of a macromolecule,⁶⁻⁸ it is clear (from Table 5) that, in the context of the present MM model, this is more difficult in the case of the FAD structures. This situation should not be surprising in view of the varying nature of the intermolecular interactions in the seven structures, plus the fact that the MM function does not take into account polarization and internal electronic structural changes resulting from intermolecular hydrogen-bonding differences (as we saw operate in the case of the ab initio $r(\text{CH})$ of free groups, and as has similarly been seen for such bonds in other molecules³⁷). To reproduce intramolecular stretching frequencies, such as C=O s, OH s, and CH s, the usual relation requires that the MM function accurately account for the respective bond length changes between the FAD structures. In current MM models, such bond length changes result from several factors that influence the force acting along the bond: intermolecular nonbonded interactions (electrostatic and van der Waals), the chosen intrinsic bond length, and the diagonal and off-diagonal harmonic and anharmonic force constants associated with the bond. Obtaining the proper balance between the parameters determining these effects is obviously a delicate process, certainly restricted by the exclusion of polarization. This is further constrained by the weights in the optimization given to reproduce the relative interaction energies and structures of the dimers, the latter being crucial to obtaining good intermolecular frequency agreement. The C–O t modes present an additional problem. We noted the desirability of choosing a different barrier height for **II** in comparison with that of the other structures, occasioned by the $\sim 300 \text{ cm}^{-1}$ spread in frequencies. A closer examination suggests that a more accurate representation would in fact correlate barrier height with the inverse of $r(\text{C–O})$. This is also physically reasonable, and indicates the kind of detail that will have to be included in MM functions of relevant systems if they are to become spectroscopically complete.

Despite these problems, the MM results are encouraging. For C=O s, the MM $r(\text{C=O})$ track the ab initio quite well (Table 7), with an rms error of 0.0013 \AA . Thus, although the C=O groups range from free (**IVB**, **VB**, **VIB**, **VII**) to strongly hydrogen bonded (**II**), the nonbonded interactions have only a small perturbing influence on $r(\text{C=O})$, perhaps because of its large force constant. The frequencies are moderately well reproduced (Table 5), and although some of the splittings, which depend strongly on the charge fluxes,⁹ are fine, others are poorly reproduced. As a result, some of the MM frequencies do not relate to their ab initio counterparts according to the relative $r(\text{C=O})$. Considering that even for free C=O groups some $r(\text{C=O})$ (**VIB** and **VII**) are very close to the monomer value of 1.2167 \AA , whereas others (**IVB** and **VB**) are not, it seems that, as in the case of CH s, the specifics of the intermolecular hydrogen-bonding interaction in the dimer can influence even an "isolated"

bond and, thus, its stretching frequency. For OH s, the situation is somewhat more complicated. In the cases of free OH groups (**IIIB**, **VIA**, **VIII**) or those with weak C–H \cdots OH interactions (**VIB**, **VII**), the MM $r(\text{OH})$ track the ab initio quite well (rms error of 0.0014 \AA). Their frequencies (Table 5) are in fairly good agreement with the ab initio and relate to these in accord with the relative $r(\text{OH})$. In a second category are OH bonds associated with strong dimer interaction energies, and hence strong hydrogen bonds (Table 1), viz. **II**, **IIIA**, **IVA**, and **IVB**: the rms error for these is 0.0107 \AA . In a separate category is **V**, perhaps because it is a doubly hydrogen-bonded OH group: its error is 0.0215 \AA . In these latter cases, although the frequencies are in accord with the relative $r(\text{OH})$, the agreement with ab initio frequencies is poor. There are at least two possible reasons for these large errors. First, the same cubic and quartic anharmonic OH force constants were used for all structures, and it is not unreasonable to believe that such force constants, which are involved in determining bond length changes, could be different for free and hydrogen-bonded OH bonds. Second, the van der Waals parameters of the hydrogen-bonded H of the OH may well be different from those of the H of a free OH; these were kept the same in these calculations, particularly because they are not well determined in the parameter refinement. At this stage, the predicted MM OH s frequencies must be considered to be in reasonable agreement with the ab initio. For C–O t, the agreement between MM and ab initio $r(\text{C–O})$ is good when the OH is free (**IIIB**, **VIA**, **VIII**) or has a weak C–H \cdots O hydrogen bond (**VIB**, **VII**) (rms error of 0.0026 \AA), and the frequency agreement is also reasonably good. In other cases (except for **II**, for which the barrier was individually optimized), the $r(\text{C–O})$ agreement is poor (rms error of 0.0063 \AA), and the frequency agreement is poorer. As we noted, this is undoubtedly a consequence of assuming a single barrier (and therefore torsion force constant) for all of these structures whereas a possible dependence on $r(\text{C–O})$ might be more reasonable. Nevertheless, despite the assumed simple barrier dependence, the trend of the ab initio frequencies is reasonably well followed.

For CH s, as we have seen, the ab initio $r(\text{CH})$ vary by 0.0017 \AA for free CH groups and by only $\sim 0.0020 \text{ \AA}$ between free and hydrogen-bonded groups. It is therefore not surprising that such small changes are difficult to reproduce (in fact, MM and ab initio $r(\text{CH})$ are anti-correlated), particularly because polarization effects (perhaps represented by changes in charges on the adjacent oxygen atoms) may be influential. Furthermore, errors in the C=O and C–O bonds will cause errors in the CH bond through the CH/C=O and CH/C–O interaction force constants, which are not small in the ab initio force field. In view of the many uncertainties, including further optimization of the van der Waals parameters, it is probably not useful to expect the current MM model to predict such fine details.

On a related matter, however, we wish to point out that, while the difference in properties of C–H \cdots O and O–H \cdots O hydrogen bonds can be shown to reside only in quantitative rather than qualitative differences in their interaction energy components, making it "difficult to conclude that there is any profound or fundamental difference between [these] interactions",³¹ in the FAD structures simple electrostatic force considerations point to $r(\text{OH})$ increasing and $r(\text{CH})$ decreasing on hydrogen bonding (Table 7). Interactions in C–H \cdots O and O–H \cdots O hydrogen bonds are weak, and can therefore be treated by perturbation methods based on electrostatic and van der Waals interactions. In the equilibrium dimer structures, intermolecular interaction forces on each atom must be balanced by intramolecular geometry changes from the monomer equilibrium structure. The

forces in Cartesian coordinates can be transformed to nonredundant internal coordinates, and the forces in these internal coordinates must vanish in the equilibrium structures. If the intermolecular interaction force on a bond, say OH, is to stretch it, then the bond must elongate in order to generate the compensating contraction force. The striking difference between CH and OH bonds in the FAD dimers is that C has a positive charge and O has a negative charge. In this context, we can inquire what effect the close O⁻ acceptor atom has on the internal forces it generates that change the C⁺-H⁺ and O⁻-H⁺ bond lengths from their equilibrium values. Using the known charges and the ab initio dimer geometries, we have calculated these forces, the interaction forces being determined mainly by interaction between the acceptor O⁻ and C⁺-H⁺ and O⁻-H⁺. In all cases, their direction is such that they would lengthen OH bonds and shorten CH bonds, with the force on OH being roughly an order of magnitude larger than that on CH. For example, for **III** the force on OH is -0.0626 mdy (negative leads to bond lengthening) while that on CH is 0.0044 mdy; for **IV** the force on OH is -0.0707 mdy and that on CH is 0.0025 mdy; for **VI** the forces on the CH bonds are 0.0046 (A) and 0.0021 (B) mdy. Of course, other interactions are involved (electrostatic interactions with other atoms, van der Waals interactions, intramolecular interactions), but the effect of the dominant electrostatic term on the hydrogen bond may be concentrated in this local intermolecular interaction.

Conclusions

Our MM energy function for the seven planar hydrogen-bonded FAD structures, which incorporates atomic dipoles and charge fluxes in addition to atomic charges and which optimizes intramolecular force constants by the analytic SDFP procedure,⁴ is shown to give good reproduction of a range of ab initio properties of this system. A common set of parameters (which would be modified to at least allow different charges and dipoles if polarization were included^{38,39}) results in rms errors of <0.3 kcal/mol in interaction energies (which range from 13.6 to 1.9 kcal/mol), <0.5 Å in translational and <20° in rotational structural parameters, and ~22 cm⁻¹ in the six intermolecular frequencies (which range from 254 to 16 cm⁻¹), and quite reasonable reproduction of intramolecular frequencies. Together with the van der Waals terms in the MM function, such a nonbonded electrostatic model provides a substantial description of the intermolecular interactions in the FAD.

This result has an important general significance for the description of spectroscopically (as well as energetically) successful hydrogen-bonding terms in MM energy functions, viz., that a covalent term may not be necessary in most cases. There has been some disagreement on this point.⁴⁰ It has been claimed that the hydrogen bond in ice is covalent, although this interpretation has been challenged.⁴¹ A study of hydrogen-bonded amides⁴² asserts that a Morse function results in a best fit to ab initio energies, although atomic dipoles were not included in the MM function. A perceptive study⁴³ shows that covalent character may be important in systems stabilized by resonance, but in other systems (the example analyzed was a chain of urea molecules) classical electrostatic interactions were able to essentially describe the hydrogen-bond interaction. This seems to be the case in the FAD, if atomic dipoles are included,¹⁻³ and the description would probably even be further improved with the inclusion of polarization. It therefore seems reasonable to conclude that the hydrogen bond contribution in most macromolecular MM energy functions can be satisfactorily accounted for by a complete nonbonded interaction description.

Acknowledgment. This research was supported by NSF Grant Nos. MCB 9903991 and DMR 9902727.

References and Notes

- (1) Qian, W.; Krimm, S. *J. Phys. Chem. A* **1997**, *101*, 5825.
- (2) Qian, W.; Krimm, S. *J. Phys. Chem. A* **1998**, *102*, 659.
- (3) Qian, W.; Mirkin, N. G.; Krimm, S. *Chem. Phys. Lett.* **1999**, *315*, 125.
- (4) Palmo, K.; Pietila, L.-O.; Krimm, S. *J. Comput. Chem.* **1991**, *12*, 385.
- (5) Palmo, K.; Pietila, L.-O.; Krimm, S. *J. Comput. Chem.* **1993**, *17*, 67.
- (6) Palmo, K.; Mirkin, N. G.; Pietila, L.-O.; Krimm, K. *Macromolecules* **1993**, *26*, 6831.
- (7) Palmo, K.; Mirkin, N. G.; Krimm, S. *J. Phys. Chem. A* **1998**, *102*, 6448.
- (8) Mannfors, B.; Sundius, T.; Palmo, K.; Pietila, L.-O.; Krimm, S. *J. Mol. Struct.* **2000**, *521*, 49.
- (9) Qian, W.; Krimm, S. *J. Phys. Chem.* **1996**, *100*, 14 602.
- (10) Turi, L. *J. Phys. Chem.* **1996**, *100*, 11 285.
- (11) Hermida Ramon, J. M.; Rios, M. A. *Chem. Phys.* **1999**, *250*, 155.
- (12) Yokoyama, I.; Miwa, Y.; Machida, K. *J. Am. Chem. Soc.* **1991**, *113*, 6458.
- (13) Moller, C.; Plesset, M. S. *Phys. Rev.* **1934**, *46*, 618.
- (14) Frisch, M. J.; Trucks, G. W.; Schlegel, H. B.; Gill, P. M. W.; Johnson, B. G.; Robb, M. A.; Cheeseman, J. R.; Keith, T.; Petersson, G. A.; Montgomery, J. A.; Ragavachari, K.; Al-Laham, M. A.; Zakrzewski, V. G.; Ortiz, J. V.; Foresman, J. B.; Cioslowski, J.; Stefanov, B. B.; Nanayakkara, A.; Challacombe, M.; Peng, C. Y.; Ayala, P. Y.; Chen, W.; Wong, M. W.; Andres, J. L.; Replogle, E. S.; Gomperts, R.; Martin, R. L.; Fox, D. J.; Binkley, J. S.; Defrees, D. J.; Baker, J.; Stewart, J. P.; Head-Gordon, M.; Gonzalez, C.; Pople, J. A. GAUSSIAN 94, Revision D. 4. Gaussian, Inc.: Pittsburgh, PA, 1995.
- (15) Mirkin, N. G.; Krimm, S. *J. Mol. Struct.(THEOCHEM)* **1995**, *334*, 1.
- (16) Tsuzuki, S.; Uchamaru, T.; Matsumura, K.; Mikami, M.; Tanabe, K. *J. Chem. Phys.* **1999**, *110*, 11 906.
- (17) Boys, S. F.; Bernardi, F. *Mol. Phys.* **1970**, *19*, 553.
- (18) Mirkin, N. G.; Krimm, S. *J. Am. Chem. Soc.* **1991**, *113*, 9742.
- (19) Bertie, J. E.; Michaelian, K. H. *J. Chem. Phys.* **1982**, *76*, 886.
- (20) Dinur, U.; Hagler, A. T. *J. Chem. Phys.* **1989**, *91*, 2949.
- (21) Decius, J. C. *J. Mol. Spectrosc.* **1975**, *57*, 348.
- (22) Dinur, U. *Chem. Phys. Lett.* **1990**, *166*, 211.
- (23) Jedlovsky, P.; Turi, L. *J. Phys. Chem. A* **1997**, *101*, 2662.
- (24) Jedlovsky, P.; Turi, L. *J. Phys. Chem. A* **1999**, *103*, 3796.
- (25) Minary, P.; Jedlovsky, P.; Mezei, M.; Turi, L. *J. Phys. Chem. B* **2000**, *104*, 8287.
- (26) Palmo, K.; Krimm, S., to be published.
- (27) Shida, N.; Barbara, P. F.; Almlöf, J. *J. Chem. Phys.* **1991**, *94*, 3633.
- (28) Derewenda, Z. S.; Lee, L.; Derewenda, U. *J. Mol. Biol.* **1995**, *252*, 248.
- (29) Bella, J.; Berman, H. M. *J. Mol. Biol.* **1996**, *264*, 734.
- (30) Chakrabarti, P.; Chakrabarti, S. *J. Mol. Biol.* **1998**, *284*, 867.
- (31) Gu, Y.; Kar, T.; Scheiner, S. *J. Am. Chem. Soc.* **1999**, *121*, 9411.
- (32) Cubero, E.; Orozco, M.; Hobza, P.; Luque, F. J. *J. Phys. Chem. A* **1999**, *103*, 6394.
- (33) Vargas, R.; Garza, J.; Dixon, D. A.; Hay, B. P. *J. Am. Chem. Soc.* **2000**, *122*, 4750.
- (34) Jeffrey, G. A. *J. Mol. Struct.* **1999**, *485-486*, 293.
- (35) Krimm, S.; Kuroiwa, K.; Rebane, T. *Conformation of Biopolymers*; Academic Press: London and New York, 1967, p 439.
- (36) Krimm, S.; Kuroiwa, K. *Biopolymers* **1968**, *6*, 401.
- (37) Thomas, H. D.; Chen, K.; Allinger, N. L. *J. Am. Chem. Soc.* **1994**, *116*, 5887.
- (38) Mannfors, B.; Palmo, K.; Krimm, S. *J. Mol. Struct.* **2001**, *556*, 1.
- (39) Mannfors, B.; Mirkin, N. G.; Palmo, K.; Krimm, S. *J. Comput. Chem.*, in press.
- (40) Isaacs, E. D.; Shukla, A.; Platzman, P. M.; Hamann, D. R.; Barbiellini, B.; Tulk, C. A. *Phys. Rev. Lett.* **1999**, *82*, 600.
- (41) Ghanty, T. K.; Staroverov, V. N.; Koren, P. R.; Davidson, E. R. *J. Am. Chem. Soc.* **2000**, *122*, 1210.
- (42) Kang, Y. K. *J. Phys. Chem. B* **2000**, *104*, 8321.
- (43) Dannenberg, J. J.; Haskamp, L.; Masunov, A. *J. Phys. Chem. A* **1999**, *103*, 7083.